AD-A114 291 MASSACHUSETTS INST OF TECH LEXINGTON LINCOLN LAB F/G 9/5
A 20 GHZ CIRCULARLY POLARIZED, FAN BEAM SLOT ARRAY ANTENNA,(U)
MAR 82 D C WEIKLE F19628-80-C-0002
UNCLASSIFIED TR-563 ESD-TR-82-001 NL

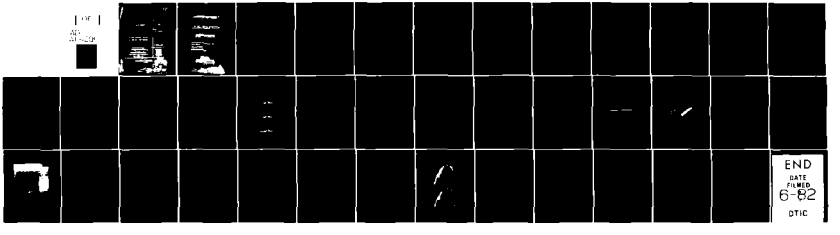

END
DATE FILMED
6-82
DTIC

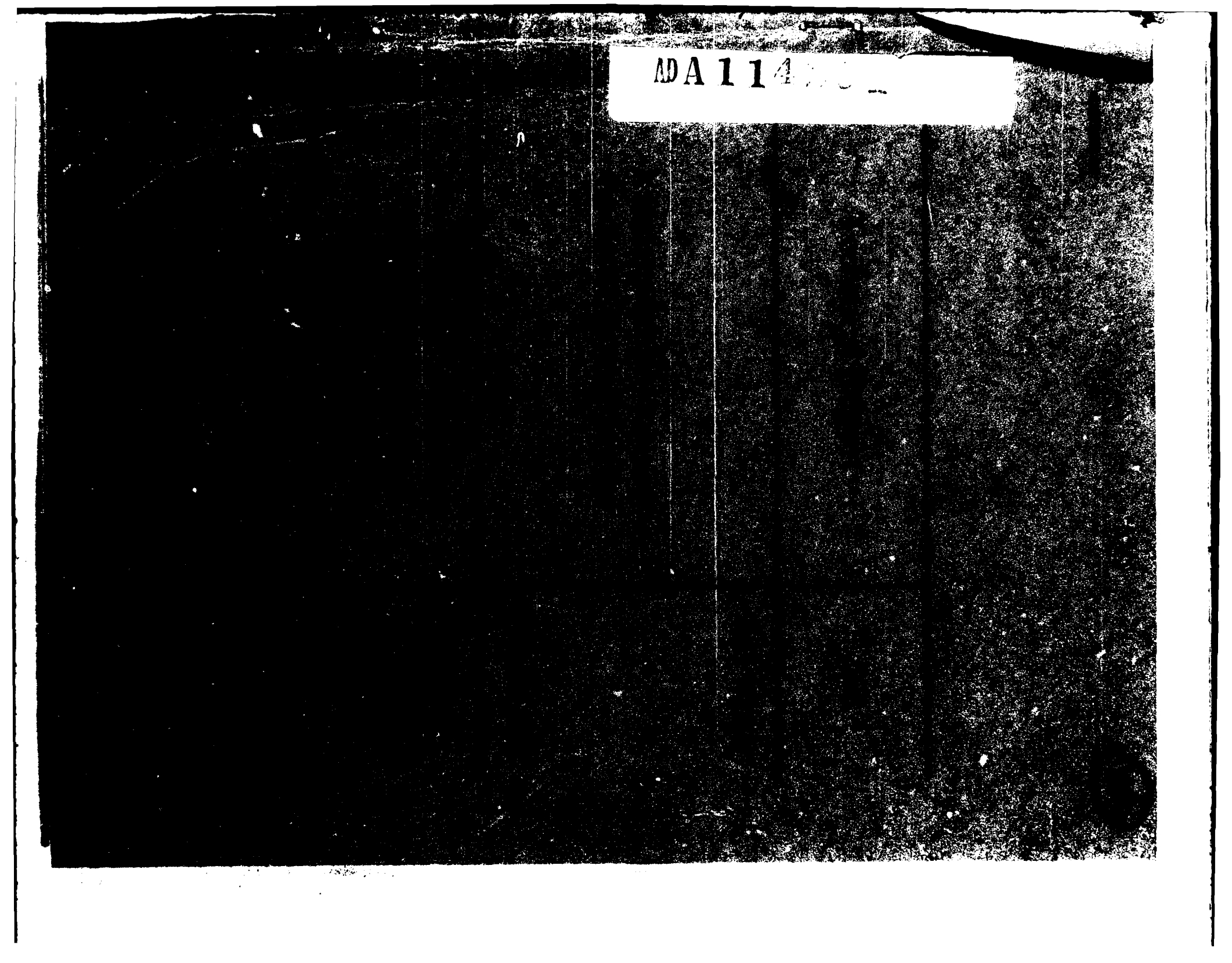
AD A 11

MASSACHUSETTS INSTITUTE OF TECHNOLOGY
LINCOLN LABORATORY

A 20 GHz CIRCULARLY POLARIZED, FAN BEAM SLOT ARRAY ANTENNA

D.C. WEIKLE
Group 61

TECHNICAL REPORT 563

9 MARCH 1982

LEXINGTON MASSACHUSETTS

ABSTRACT

An EHF waveguide slot array was developed for possible use as a receive-only paging antenna for ground mobile terminals. The design, fabrication, and measured performance of this antenna are presented. The antenna generates a circularly polarized fan beam that is narrow in azimuth and broad in elevation. When mechanically rotated in azimuth, it can receive a 20-GHz satellite transmission independent of mobile terminal direction. Azimuth plane sidelobe levels, which are typically <-40 dB from the main lobe, provide for discrimination against ground and airborne jammers.

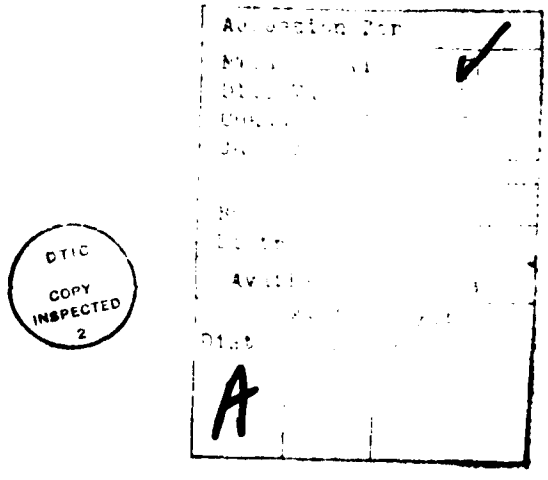

CONTENTS

	Abstract	iii
	List of Illustrations	vi
I.	INTRODUCTION	1
II.	DEVELOPMENT	2
	A. Waveguide Slot Array	2
	B. Circular Polarizer	14
III.	PERFORMANCE	19
	A. Radiation Patterns	19
	1. Linear Array	19
	2. Circularly Polarized Array	24
	3. Circularly Polarized Array on Ground Plane	24
	B. Impedance	24
	C. Gain	29
IV.	CONCLUSIONS	31
Acknowledgments		32
References		32

ILLUSTRATIONS

1.	Slotted waveguide section.	5
2A.	12-in. slot array parallel plate fixture.	6
2B.	12-in. slot array parallel plate fixture (sectional side view).	6
3.	Graph of slot angle vs. depth of cut.	7
4.	Graph of coupling vs. slot angle.	9
5.	±90° theoretical E-plane pattern: (a) at 20.2 GHz, (b) at 20.45 GHz, (c) at 20.7 GHz.	11
6.	±20° theoretical E-plane pattern: (a) at 20.2 GHz, (b) 20.45 GHz, (c) at 20.7 GHz.	12
7.	Table of slot angle and depth of cut for array 1 and 2.	13
8.	24-in. slotted waveguide.	15
9.	24-in. slotted waveguide section between parallel plates (sectional side view).	16
10.	24-in. array.	17
11.	Circularly polarized array.	18
12.	Summary of array measurements.	20
13.	Antenna positioner.	21
14A.	Typical azimuth (E-plane) pattern - linear array.	22
14B.	Typical elevation (H-plane) pattern - linear array.	22
15.	Cross-polarized azimuth pattern - linear array.	23
16.	Typical vertical polarization pattern - circularly polarized array.	25
17.	Typical azimuth polarization pattern - circularly polarized array.	26
18.	Sketch of circularly polarized array over ground plane.	27
19.	Array over ground plane, θ=45°: (a) without absorber, (b) with absorber.	28
20.	VSWR - linear and circularly polarized array.	30

I. INTRODUCTION

A possible requirement for a ground mobile terminal is the capability of receiving a 20-GHz "call-up" (paging) satellite transmission while the vehicle is in motion. Since the vehicle is in motion, the azimuth to the satellite is constantly changing. An antenna which is omnidirectional in azimuth would be able to receive the satellite signal independent of vehicle direction. However, the omnidirectional pattern, having a low gain, requires excessive satellite EIRP (effective isotropic radiated power) and also provides no discrimination against ground and airborne jammers. An alternative approach is a fan beam antenna with a pattern that is narrow in azimuth and wide in elevation. The antenna must then be rotated in azimuth to scan the complete hemisphere. One antenna suitable for providing a fan beam is a waveguide slot array. This report deals with the development of such an array.

The design goals of the proposed antenna are listed below:

Center Frequency	20.45 GHz
Bandwidth	500 MHz
Gain	~ 25.0 dBi
Azimuth Half-Power Beamwidth	1.75^{o}
Azimuth Sidelobe Level	30 dB below main lobe
Elevation Half-Power Beamwidth	70^{o}
Input VSWR	<1.5
Antenna Width	~ 24 inches

II. DEVELOPMENT

A. Waveguide Slot Array

The array design problem consists of (1) determining the excitation coefficients of the individual slots to achieve the required performance, and (2) determining the slot dimensions, spacing, and angle of inclination to achieve the required excitation coefficients and input VSWR. A computer program was generated to aid in solving these problems. The program is designed to compute the individual element excitation coefficients for a given number of slots and a specified amplitude distribution. By specifying the conductance of the last element (program input parameter), the conductance values of the preceding elements are calculated to yield the specificed distribution. The program also computes the resultant input VSWR of the array and the unradiated power dissipated in the load. Element spacing, waveguide attenuation, and dimensions are parameters included in the computations. After the design parameters are chosen, a theoretical E-plane antenna pattern is plotted.

A resonant array (element spacing = $\lambda g/2$, where λg = guide wavelength) was initially considered to determine if it was capable of providing a matched condition over the required 2.5% band. The computations revealed that although the antenna would be well matched at the center frequency (20.45 GHz), the input VSWR would quickly deteriorate and would not support the necessary bandwidth. Consequently, it was necessary to use a nonresonant array (spacing slightly smaller or larger than $\lambda g/2$) to provide the impedance bandwidth required. Unlike the resonant array, which radiates a broadside beam, the nonresonant array beam peak position is skewed from broadside and its skew angle is frequency dependent. As the frequency is increased, the beam moves toward the load end of the array. Since the paging antenna is intended to be rotated continuously, this effect is expected to be of little consequence, as long as the skew angle is small.

To determine the element spacing, two factors, the input impedance and the skew angle, must be considered. The expression which relates the skew angle (θ) to element spacing (ℓ) is given by[1]

$$\sin\theta = \frac{\lambda}{\lambda g} - \frac{\lambda}{2\ell} \qquad (1)$$

where λg = guide wavelength

λ = free-space wavelength

This expression shows that the more the element spacing deviates from $\lambda g/2$, the larger the skew angle. However, when the element spacing approaches $\lambda g/2$ ($\theta \sim 0^{o}$), the discontinuities created by the individual elements are in phase and an increase in input VSWR results. Interelement spacing of 0.43 inches (0.54 λg) was computed to be the minimum spacing for acceptable VSWR over the frequency band. With this spacing, the calculated skew angle varies from 2.2^{o} to 4.1^{o} over the band. At this spacing, 56 elements are necessary, and thus a 24-inch aperture is required to provide the desired azimuth beamwidth and gain.

For ease of manufacturing, inclined slots in the narrow waveguide wall (edge slots) were selected*. Since the narrow dimension of the waveguide is substantially less than the half free-space wavelength required for the slot to resonate, the slot must be extended into the broad dimension of the waveguide to obtain the required length. To determine this resonant length (and, therefore, the depth of cut into the top and bottom walls of the waveguide) for a given angle of inclination, a series of 12-inch test arrays were built**. The first of this series was an array of 20 5^{o} slots (i.e.,

*Any linear polarization was satisfactory at this point, since it was intended to add an external polarizer to the array.

**To keep the waveguide dimensionally consistent in each array, all the waveguide sections were supplied exclusively from one 10-foot length.

inclined at 5°) cut at 0.43-inch spacing into the narrow wall of WR-42 copper waveguide. (The reason for using a large number of slots will become evident later.) The slots were cut with alternating positive and negative inclinations (see Fig. 1) to enable the radiated fields of the slots to be in phase at ~$\lambda g/2$ spacing. The test array was then placed between parallel plates to simulate the environment in the final design (see Figs. 2A and 2B). The separation between the parallel plates (0.42 inches) was chosen to provide the necessary elevation beamwidth as well as being within the confines of supporting only the TE_{10} mode over the operating frequency range. The exit aperture of the parallel plate medium was fitted with a sliding matched load which was made from 1/4-inch free space absorber (see Fig. 2B). This load minimized reflections from the parallel-plate aperture during the measurements of slot coupling.

For a particular depth of cut and a specific angle of inclination of the slot, a resonant frequency exists at which maximum power will be radiated from the slots. By roughly choosing a slot dimension (~1/2 free-space wavelength) for a resonant frequency that is slightly higher than desired, several cutting and measuring operations can be made on the same test array to establish the resonant length at the desired frequency. Swept frequency attenuation measurements were made of the insertion loss through the array of 5^{o} slots to determine the resonant frequency. Although sliding the load in the exit aperture affected the swept frequency response, the frequency at which the maximum attenuation occurred was accurately determined to be the resonant frequency. After several iterations, the resonant length was determined. This process was repeated for four other test arrays having slot inclination angles of 10^{o}, 15^{o}, 20^{o}, and 30^{o}. After the slot depth for each test array was carefully measured, a graph of slot angle vs depth of cut was generated (see Fig. 3).

The test arrays were also used to establish the coupling for a given slot angle. Accurate insertion loss measurements were made on each of the five test arrays at the resonant frequency. The measurement accuracy is

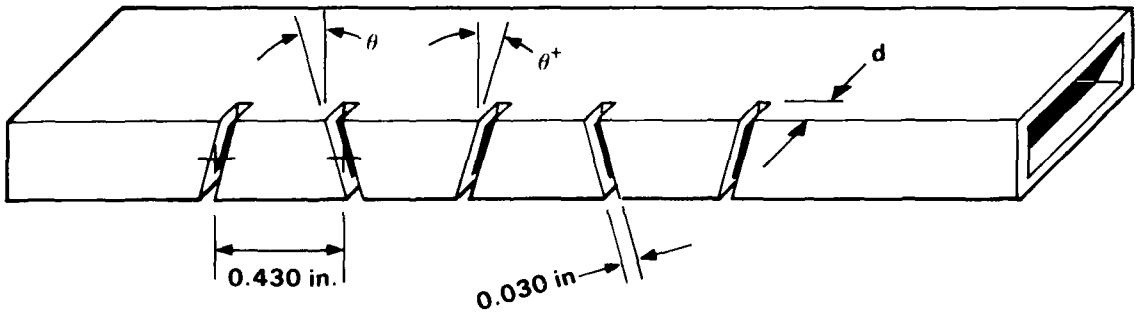

"d" - DEPTH OF CUT
θ - ANGLE OF INCLINATION

114413-N

Fig. 1. Slotted waveguide section.

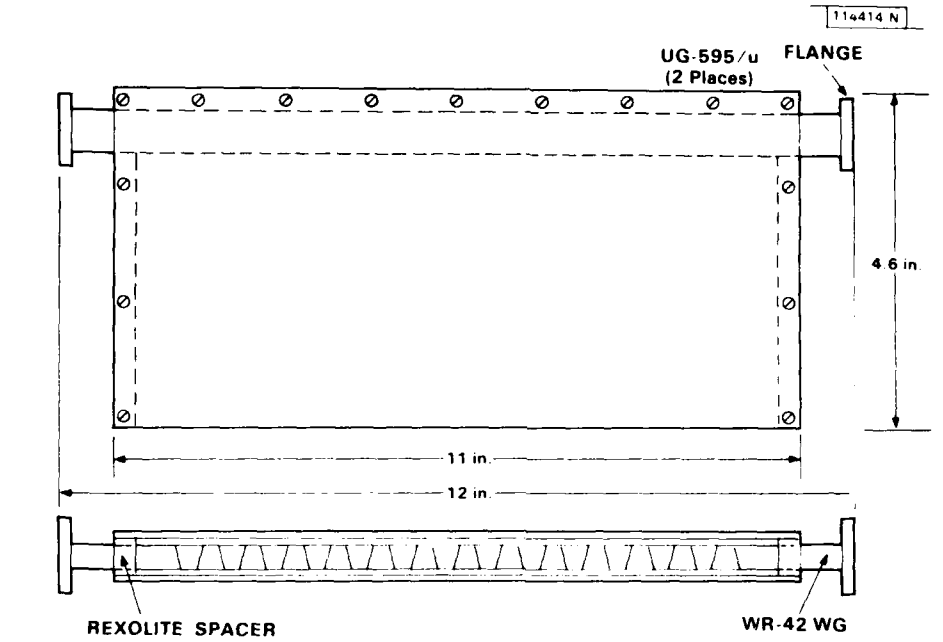

(a)

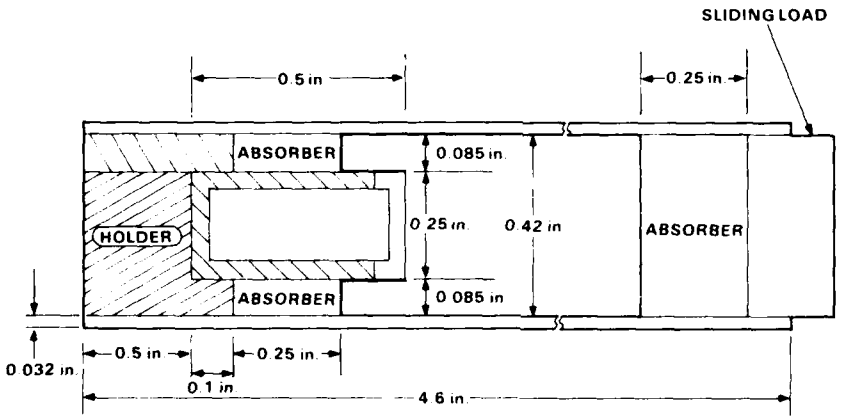

SECTIONAL SIDE-VIEW

(b)

Fig. 2. (a) 12-in. slot array parallel plate fixture, (b) sectional side view.

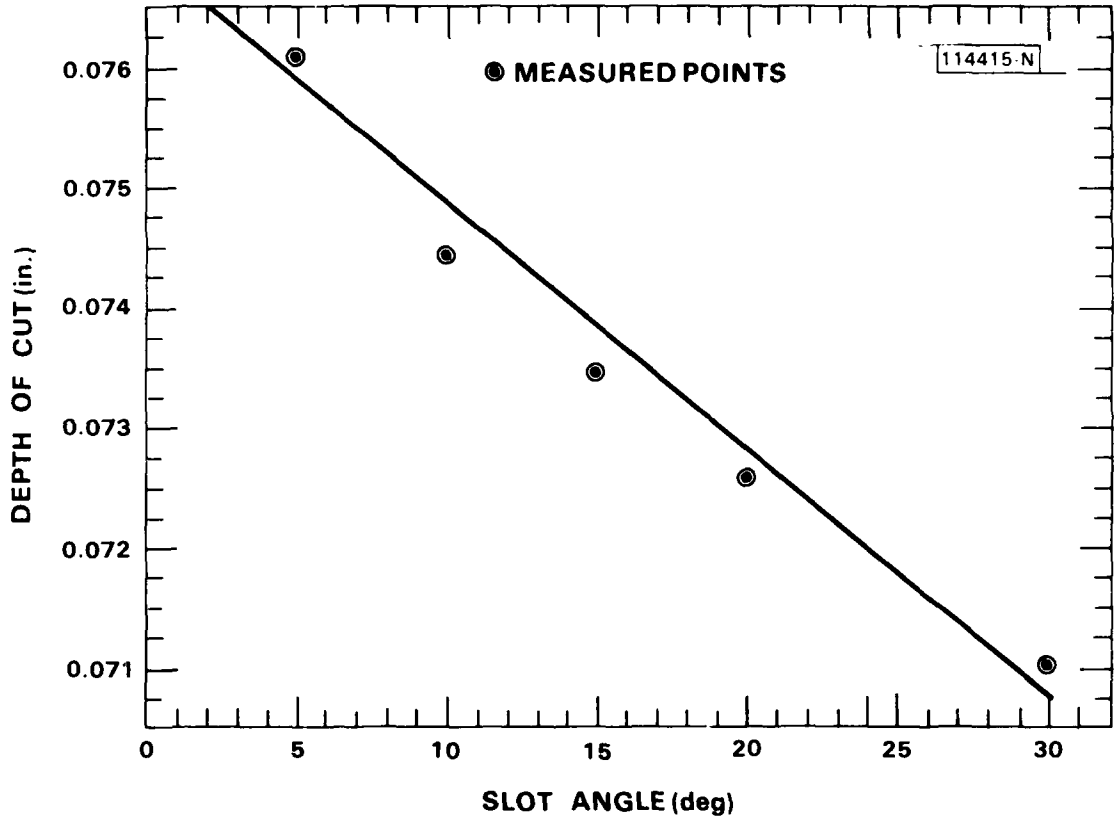

Fig. 3. Graph of slot angle vs. depth of cut.

significantly improved by using more slots (20). The insertion loss may be related to the coupling of the slot by:

$$L = 10\log (1-C)^n \tag{2}$$

therefore,

$$C = 1 - 10^{\frac{L}{10n}} \tag{3}$$

where L = measured insertion loss (dB)*
C = coupling ratio
n = number of slots

A graph of slot angle of inclination vs. coupling was plotted from the measured data (see Fig. 4). The mutual coupling effects are accurately taken into account by the large number of slots measured (20 in this case). In agreement with theory, the coupling (equal to the normalized conductance) follows a $k \sin^2\theta$ curve, where k is a constant determined empirically, and θ is the angle of the slot[2]. When the proper constant is determined (k=0.894 in this case), the $k \sin^2\theta$ expression is used to compute the specific slot angles that will produce the required distribution.

The excitation coefficients of the individual slots were computed to satisfy a Dolph-Tchebyscheff distribution. This distribution was chosen because it will produce the lowest sidelobe level for a given beamwidth. Also, this distribution can be computed in terms of the sidelobe level. The sidelobe level was specified at -50 dB to compute the excitation coefficients. This level was chosen because the measured sidelobe level is usually 10 dB or so higher than the theoretical value because of

*The waveguide insertion loss was small compared with the coupling insertion loss and, therefore, was ignored in the computations.

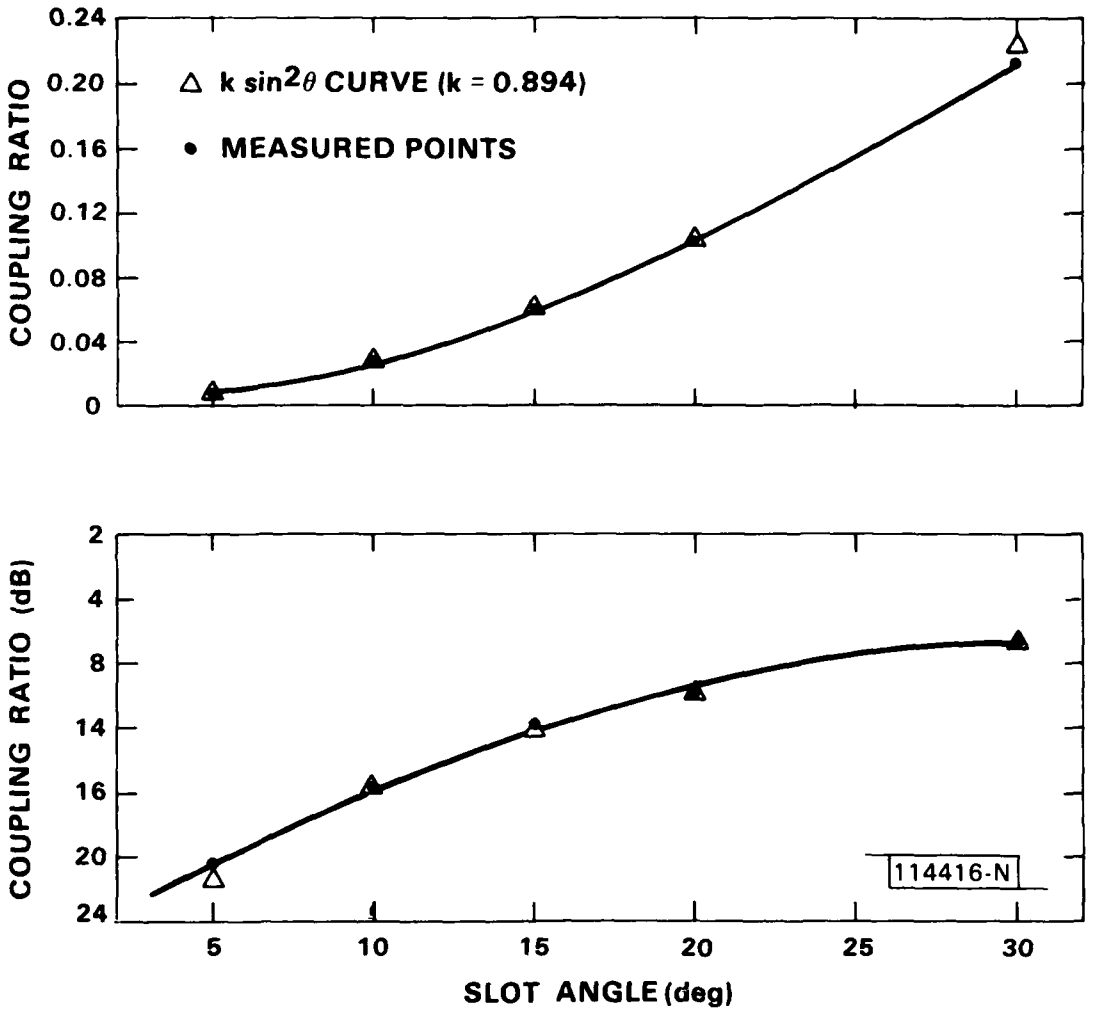

Fig. 4. Graph of coupling vs. slot angle.

implementation inaccuracies. The actual coefficients were computed using the van der Maas[3] approximation, which is an aid in computing coefficients of large arrays. The slot inclination angles were computed to achieve the required excitation coefficient by selecting the conductance value of the last element. This value must be selected within definite bounds. If the value is chosen too small, more power than necessary will be dissipated in the load, thereby making the antenna less efficient. If the value is chosen too high, the conductance values in the middle of the array will be unachievably large. The conductance value of the 56th element that best satisfied these conditions was .01. This value will produce a matched condition over the required bandwidth, and restrains the maximum required slot angle to less than 20° and the power dissipated in the load to 5.5% (0.25 dB loss).

Theoretical E-plane patterns were plotted consistent with design parameters previously mentioned. Plots over an angular range of $\pm 90^{\circ}$ are illustrated in Figs. 5A, 5B, and 5C. Figures 6A, 6B, and 6C are expanded plots with identical input parameters over a reduced angular range of $\pm 20^{\circ}$. A listing of the input parameters is located in the upper left-hand corner of each plot. It can be seen from the plots that the calculated 3 dB beamwidth is 1.9°, which is slightly larger than the 1.75° required. The sidelobe levels are more than 40 dB down. The skew angle varies from 2.2° at 20.2 GHz to 4.1° at 20.7 GHz.

The fabrication process began by generating a table of angle and depth of cut for each of the 56 elements in the array for two separate arrays. Array 1 sets the last element conductance value to 0.01 which restricts the angles to $<20^{\circ}$. Array 2, was designed with a conductance value of 0.006 for the last element which restricts the angles to $<17^{\circ}$ (see Fig. 7). Both arrays 1 and 2 were built to compare their electrical performance. Each array consists of a 27-inch length of WR-42 copper waveguide with 56 slots machined into the narrow waveguide wall. The slot machining process, which was performed on a numerically controlled milling machine, produced the accuracies required in the depth and angle of cut in each of the 56 slots. The waveguide section at

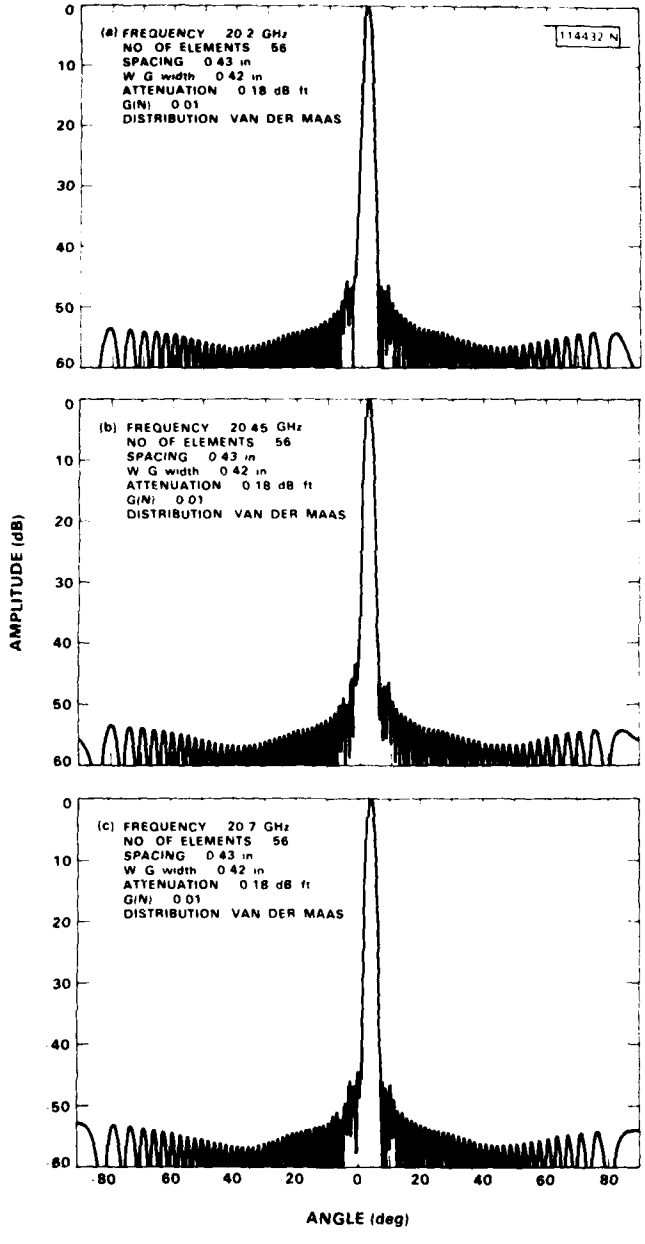

Fig. 5. ±90° theoretical E-plane pattern: (a) at 20.2 GHz, (b) at 20.45 GHz, (c) at 20.7 GHz.

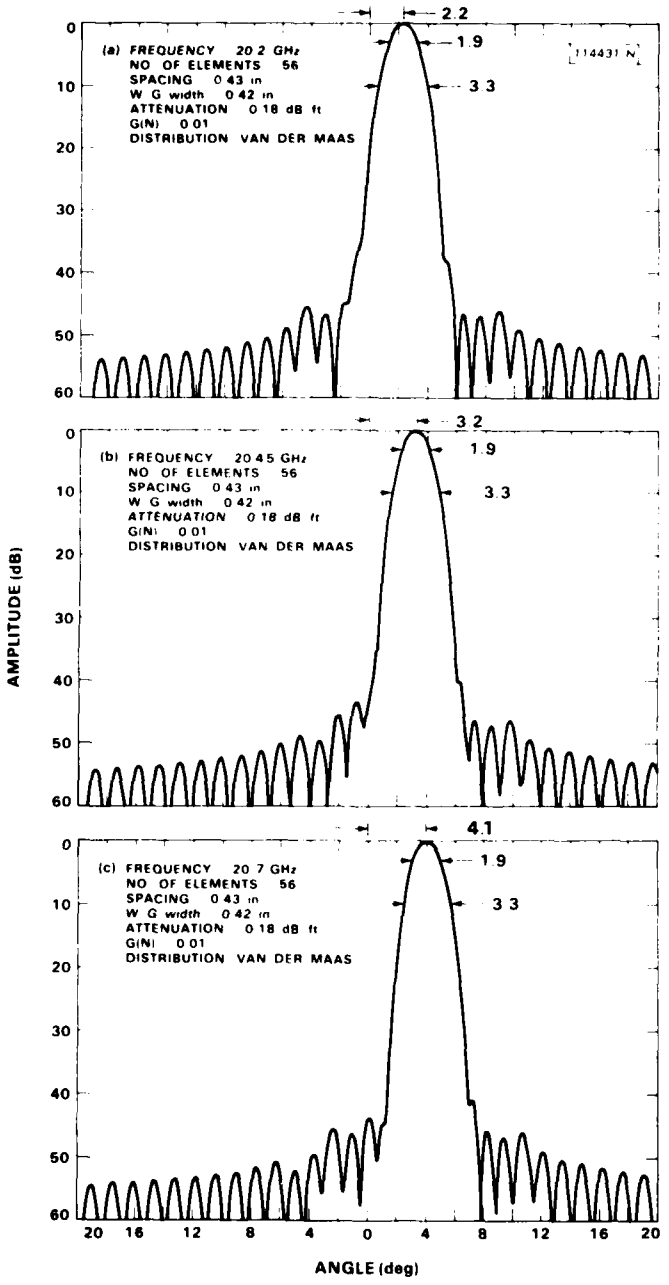

Fig. 6. ±20° theoretical E-plane pattern: (a) at 20.2 GHz, (b) at 20.45 GHz, (c) at 20.7 GHz.

ARRAY NO. 1 G(56) = 0.010			ARRAY NO. 2 G(56) = 0.006		
SLOT NO.	INCLINATION ANGLE	DEPTH OF CUT	SLOT NO.	INCLINATION ANGLE	DEPTH OF CUT
1	+2 9374	- 0761	1	+2 7227	- 0761
2	-3 0471	- 0761	2	-2 8243	- 0761
3	+3 4624	- 0760	3	+3 2088	0760
4	-4 0798	- 0758	4	3 7804	0759
5	+4 6193	- 0758	5	+4 2795	0758
6	-5 1731	- 0756	6	-4 7913	0757
7	+5 7385	- 0755	7	+5 3133	- 0756
8	6 3154	- 0754	8	5 8453	0755
9	+6 9016	- 0752	9	+6 3849	0753
10	-7 4969	0751	10	6 9319	0752
11	+8 0990	- 0750	11	+7 4838	0751
12	8 7064	- 0748	12	8 0391	0750
13	+9 3173	0747	13	+8 5956	0750
14	9 9305	- 0746	14	9 1519	0748
15	+10 5433	- 0745	15	+9 7052	0746
16	11 1539	0743	16	-10 2535	- 0745
17	+11 7597	0742	17	+10 7940	0744
18	-12 3598	0741	18	-11 3254	0743
19	+12 9521	- 0739	19	+11 8455	0742
20	-13 5356	- 0738	20	12 3529	- 0741
21	+14 1086	0737	21	+12 8457	0740
22	-14 6711	- 0736	22	-13 3232	0739
23	+15 2204	0735	23	+13 7825	0738
24	-15 7551	0733	24	14 2218	- 0737
25	+16 2726	0732	25	+14 6381	0736
26	16 7693	- 0731	26	-15 0277	0735
27	+17 2410	- 0730	27	+15 3866	- 0734
28	-17 6828	0729	28	15 7103	0734
29	+18 0899	0728	29	+15 9945	0733
30	-18 4573	0728	30	-16 2353	- 0732
31	+18 7802	- 0727	31	+16 4290	- 0732
32	19 0546	0726	32	16 5727	0732
33	+19 2772	- 0726	33	+16 6641	- 0732
34	-19 4443	0726	34	16 7011	- 0731
35	+19 5524	0725	35	+16 6813	- 0731
36	19 5956	0725	36	-16 6013	- 0732
37	+19 5691	- 0725	37	+16 4588	- 0732
38	-19 4641	- 0726	38	-16 2491	0732
39	+19 2730	- 0726	39	+15 9692	0733
40	18 9876	0727	40	15 6162	- 0734
41	+18 6039	- 0727	41	+15 1907	0735
42	18 1188	0728	42	14 6935	- 0736
43	+17 5360	0730	43	+14 1302	0737
44	16 8628	0731	44	-13 5074	- 0738
45	+16 1100	0733	45	+12 8340	0740
46	15 2879	- 0734	46	-12 1176	- 0741
47	+14 4074	0736	47	+11 3663	- 0743
48	-13 4774	0738	48	10 5867	0744
49	+12 5079	0740	49	+9 7867	0746
50	11 5035	0742	50	8 9700	0748
51	+10 4738	0745	51	+8 1441	0750
52	9 4252	0747	52	7 3131	0751
53	+8 3709	0749	53	+6 4860	0753
54	7 3227	0751	54	-5 6696	0755
55	+6 2885	0754	55	+4 8678	0757
56	6 0711	0754	56	4 6991	0757

114417 N

Fig. 7. Table of slot angle and depth of cut for array 1 and 2.

this stage of fabrication can be seen in Fig. 8. The waveguide section was then placed between parallel plates in the configuration shown in Figs. 9 and 10. The absorber placed on the broad walls of the waveguide, as indicated in Fig. 9, is intended to dissipate any power reflected from the exit aperture.

8. Circular Polarizer

A conventional parallel plate polarizer converts a linearly polarized plane wave into a circularly polarized wave by using of rectangular vanes (plates) oriented at 45° to the incident electric field. The spacing and length of the vanes is chosen to introduce a 90° difference in phase of waves propagating parallel and perpendicular to the vanes, thus converting the linearly polarized wave to a circular[5,6] wave. A polarizer of this type, which attaches to the exit aperture of the array, was developed, although it differs somewhat from the planar circular polarizer. It consists of 32 vanes of 0.062-inch sheet aluminum that are spaced 0.748-inch apart by means of a holder (see Fig. 11). Since the array (a line source) radiates a cylindrical wave, the inner and outer contours of the individual vanes are curved to conform to the cylindrical wave. The inner contour of the vanes is derived as the intersection of a 45° inclined plane with a right circular cylinder, therefore, it is semielliptical and the major axis of the ellipse is normal to the direction of propagation. The outer contour is derived from the inner contour that is concentric to, and 0.675 inch larger than, the inner ellipse. This design was found to produce a better ellipticity ratio and less distortion of the radiation patterns in the elevation plane than an alternative planar polarizer design.

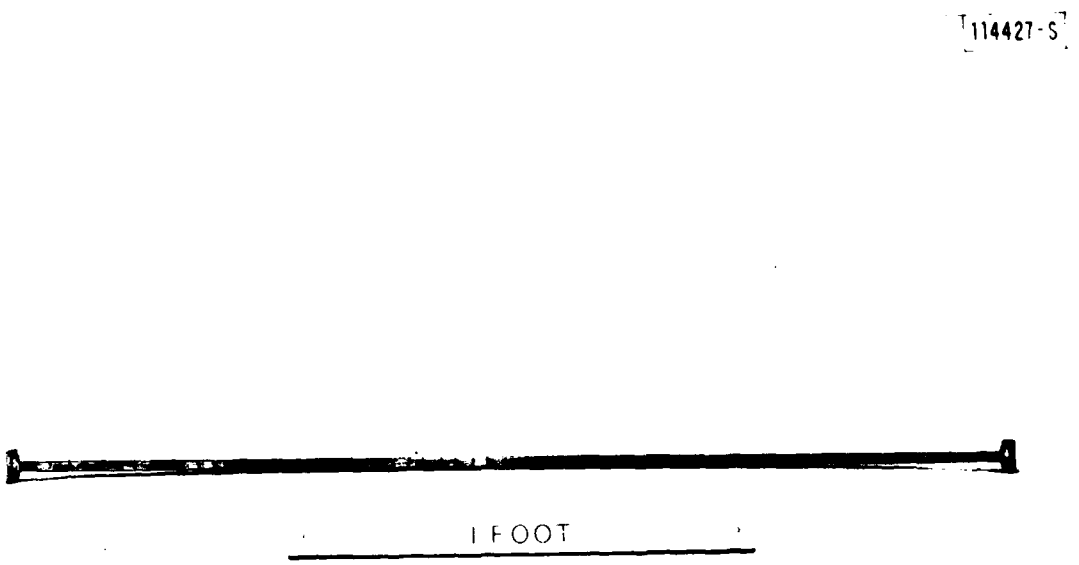

Fig. 8. 24-in. slotted waveguide.

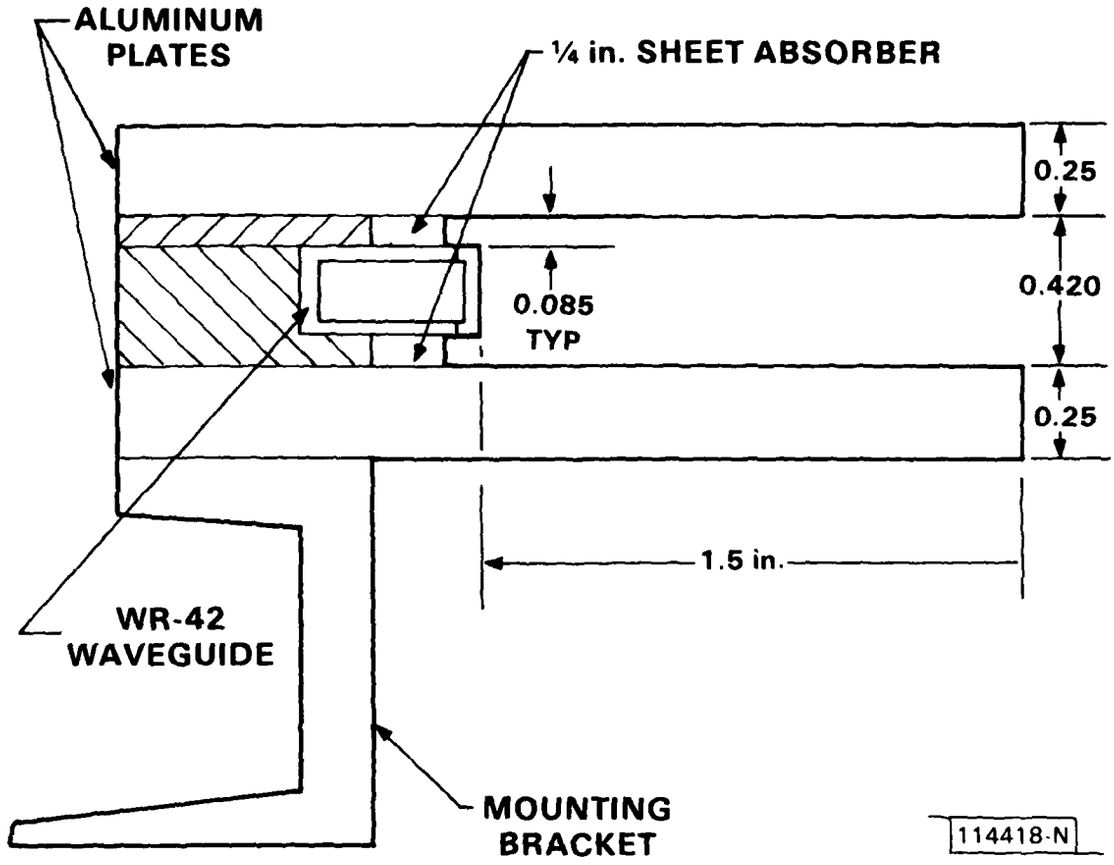

Fig. 9. 24-in. slotted waveguide section between parallel plates (sectional side view).

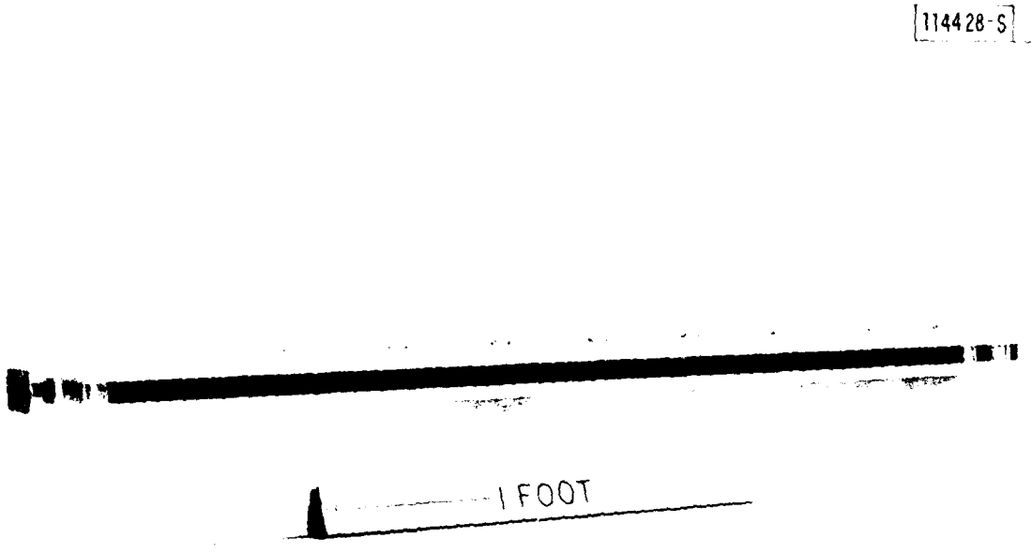

Fig. 10. 24-in. array.

114429-S

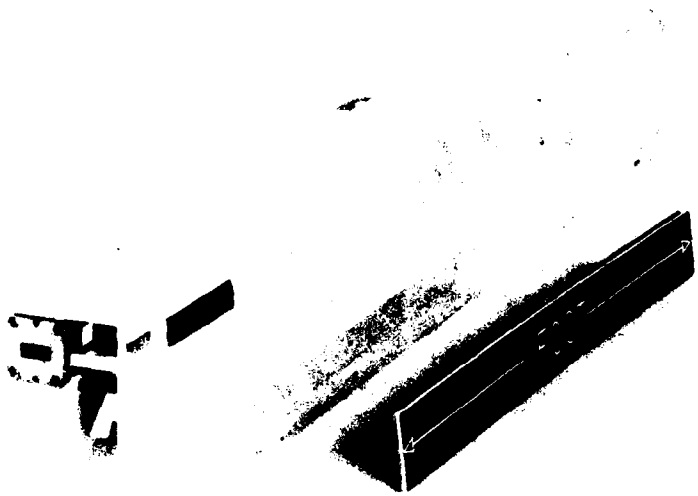

Fig. 11. Circularly polarized array.

III. PERFORMANCE

The measured performance of the array is summarized in Fig. 12. Some of the details of these measurements are described in the following sections.

A. Radiation Patterns

The radiation patterns presented in this section were measured on the 2000-ft. ground reflection range at the Lincoln Laboratory Antenna Test Range facility. The test array, which in every case was operating in the receive mode, is rotated to produce the desired patterns by means of an azimuth-over-elevation-over-azimuth positioner (see Fig. 13). Patterns were measured at three discrete frequencies over the band (20.2, 20.45, and 20.7 GHz), with and without the circular polarizer. Also, the array with polarizer was measured over a metal ground plane (20.45 GHz only), to simulate the environment of a paging antenna mounted on top of a mobile vehicle.

1. Linear Array

Figures 14A and 14B represent of the measured radiation patterns of arrays 1 and 2 without polarizer across the 500-MHz band. The particular measurements illustrated, which were taken at 20.45 GHz on array 1, reveal a half-power beamwidth of 1.56° and sidelobe levels that are greater than 30 dB down (except for the first sidelobe) and typically greater than 40 dB down from the main lobe. In the H-plane the measured half-power beamwidth is 64°. The 3-dB azimuth beamwidth is approximately 18% narrower and the sidelobe levels are about 10 dB higher than computed (see Fig. 5B). Their effects are apparently caused by an aperture distribution with somewhat less taper than planned. Additional theoretical radiation patterns generated up to 21.2 GHz, which indicates that the upper end of the band could be increased to this frequency without any major degradation in performance.

An unwanted characteristic of an edge slot waveguide array is that it radiates a strong cross-polarized component in the E-plane approximately ±45° from the main beam[4]. A radiation pattern (Fig. 15) to measure this effect revealed a component located ±42° at a level 16 dB down from the main beam. This effect compromises somewhat the antijamming capability of the array, although it is considered minor because the beamwidth of the lobe is so

	MEASUREMENT SUMMARY	20.2 GHz ARRAY NO. 1	20.2 GHz ARRAY NO. 2	20.2 GHz THEOR.	20.45 GHz ARRAY NO. 1	20.45 GHz ARRAY NO. 2	20.45 GHz THEOR.	20.7 GHz ARRAY NO. 1	20.7 GHz ARRAY NO. 2	20.7 GHz THEOR.
LINEAR ARRAY	GAIN (dBi)	23 9	23 5	—	24 1	23 3	—	24 1	23 1	—
	E-PLANE									
	3 dB BEAMWIDTH (deg)	1 62	1 68	1 9	1 56	1 55	1 9	1 53	1 50	1 9
	10 dB BEAMWIDTH (deg)	2 76	2 82	3 3	2 76	2 70	3 3	2 73	2 67	3 25
	SKEW ANGLE (deg)	2 43	2 43	2 2	3 3	3 3	3 2	4 15	4 15	4 1
	ANGLE 30 dB SIDELOBES*	6 84	5 46	2 8	4 32	4 14	2 8	5 16	5 52	2 5
	H-PLANE									
	3 dB BEAMWIDTH (deg)	65	64 5	--	64	66	--	65 5	65	—
	10 dB BEAMWIDTH (deg)	118	119 5	--	118	119	--	119	118	—
	VSWR (20 2 20 7 GHz)	1 08 (Theor 1 02)								
	PWR TO TERM (20 2 20 7 GHz)	ARRAY NO 1 7 2% (Theor 5 5%) ARRAY NO 2 12 6% (Theor 11 3%)								
CIRCULARLY POLARIZED ARRAY NO 1	GAIN (20 45 GHz)	22 3 dBi								
	ON-AXIS AXIAL RATIO (20 2 20 7 GHz)	2 5 dB								
	MAX H-PLANE AXIAL RATIO FROM 30 TO +30 (20 2 20 7 GHz)	3 0 dB								
	E PLANE SIDELOBE LEVELS (20 45 GHz)	TYPICALLY 30 dB MINOR LOBES TO 14 dB								
	VSWR (20 2 20 7 GHz)	1 12								

*BEYOND THE SPECIFIED ANGLE (From Main Beam) SIDELOBE LEVELS 30 dB and TYPICALLY 40 dB

114419-N

Fig. 12. Summary of array measurements.

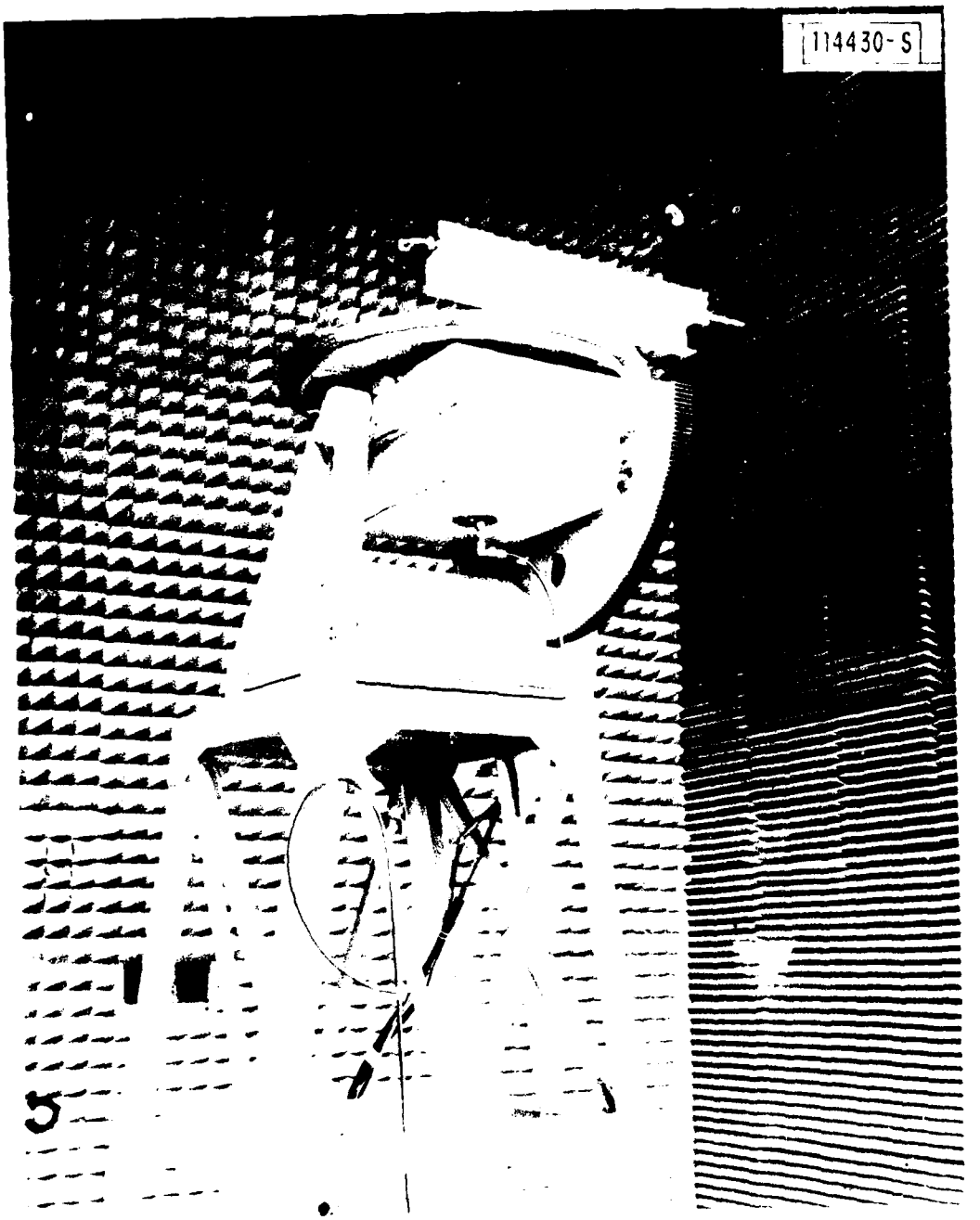

Fig. 13. Antenna positioner.

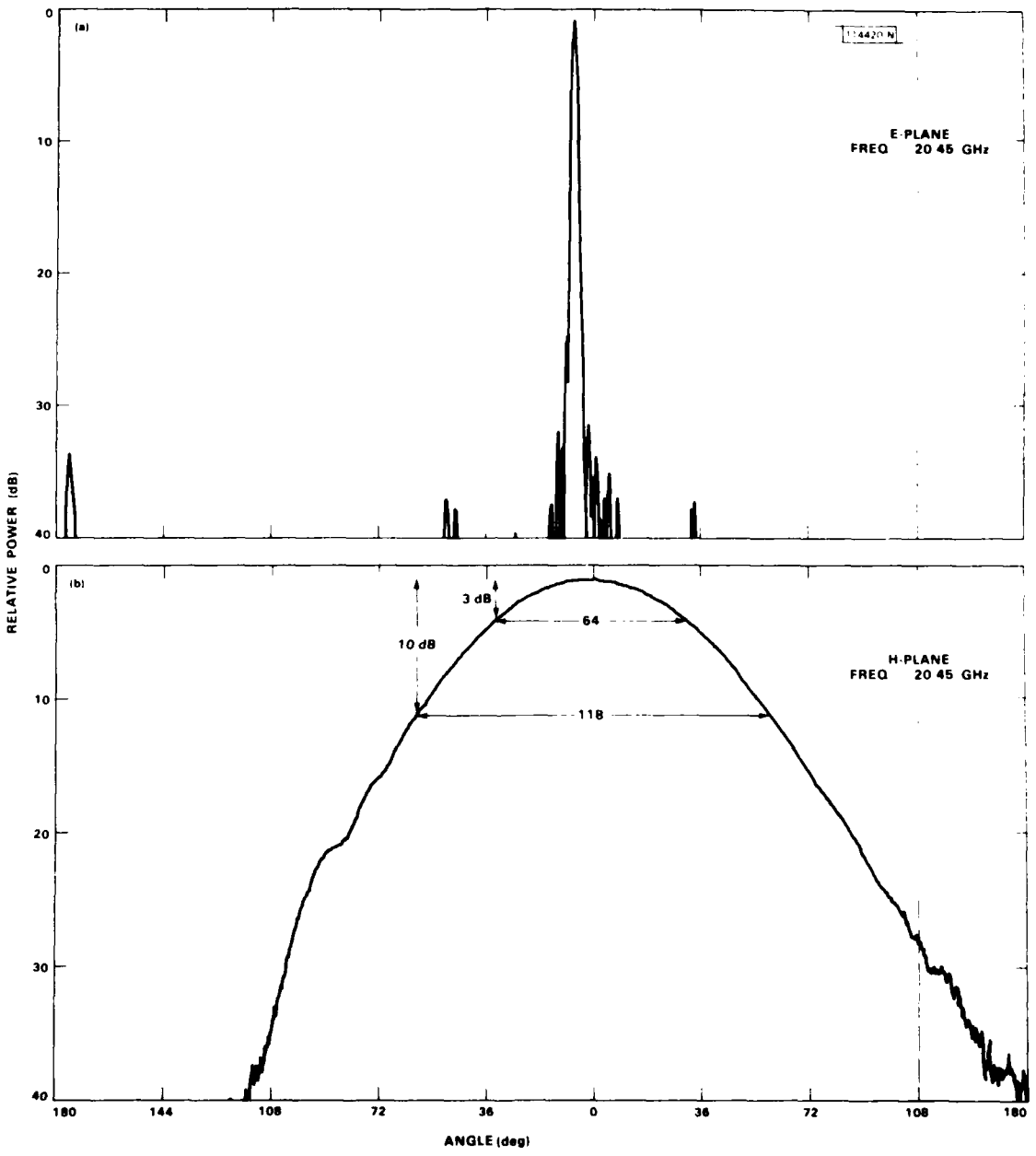

Fig. 14. (a) Typical azimuth (E-plane) pattern - linear array. (b) Typical elevation (H-plane) pattern - linear array.

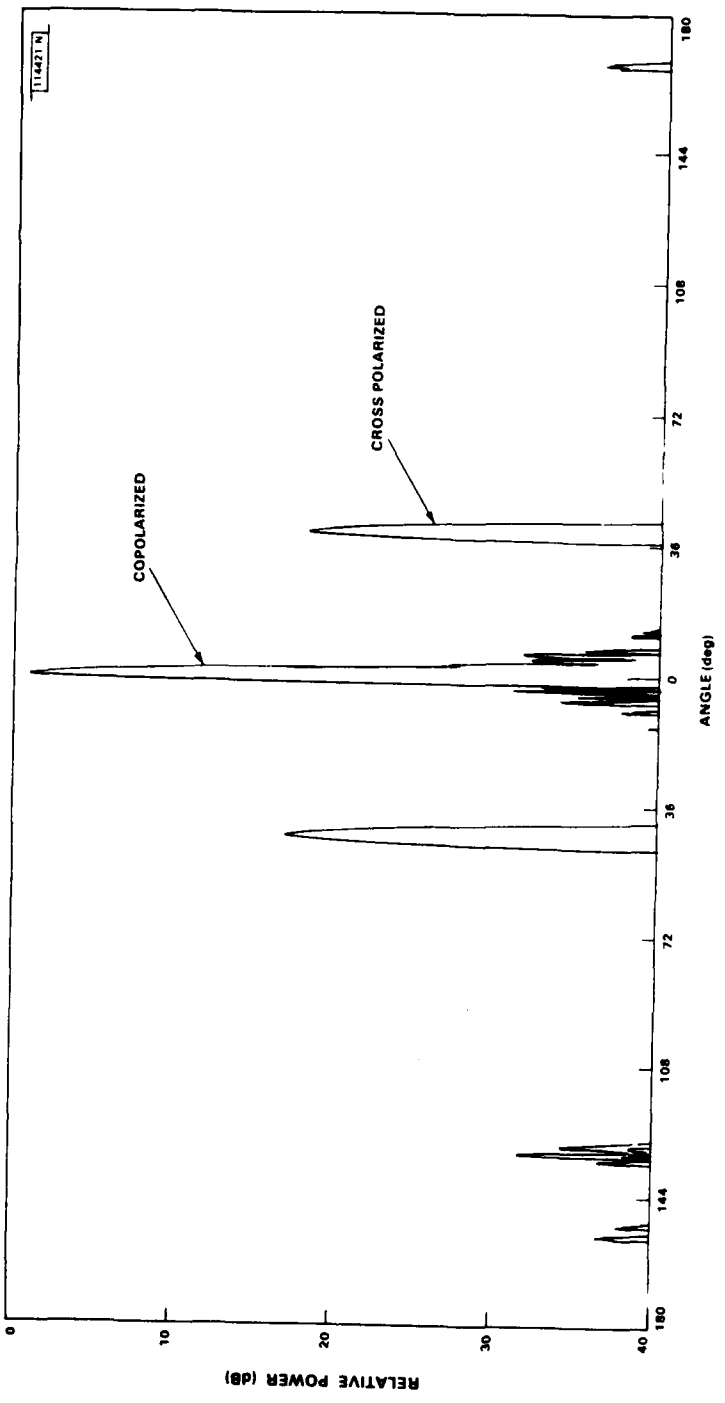

Fig. 15. Cross polarized azimuth pattern - linear array.

narrow. Cross polarization vane suppressors could be added between the slots to reduce this effect but were not felt to be necessary for this application.

2. Circularly Polarized Array

Similar patterns, as with the array alone, were measured of the array with circular polarizer (see Figs. 18A and 18B). The method used to generate the polarization patterns (axial ratio as a function of angle) was to continuously spin, in polarization, the linear source antenna while recording the desired pattern. For convenience of analyzing the polarizer, the E- and H-plane principal plane cuts, which were taken with a stationary source antenna, were overlayed onto the polarization pattern. Patterns in the elevation plane (Fig. 16) indicate an axial ratio of approximately 3 dB over the angular range of ±30°. The polarizer performs as well as can be expected at angles greater than 18° from the main beam, considering the beamwidth difference in the vertical E- and H-plane. The azimuth polarization patterns (see Fig. 17) reveal a deterioration of the sidelobe structure especially in the area of the cross-polarized component at ±42° from the main beam. These detrimental effects are attributed to reflections from the polarizer vanes at the exit aperture.

3. Circularly Polarized Array on Ground Plane

A 2x2-foot aluminum ground plane was attached to the array as shown in Fig. 18 to simulate the top of a vehicle on which the antenna might be mounted. Elevation polarization patterns were measured at 20.45 GHz for three separate angular positions of the array to the ground plane (θ=30°, 45°, 60°), and with and without the ground plane covered with absorber. The measured patterns (Figs. 19A and 19B) reveal an interference between the direct signal and reflected signal from the ground plane. As might be expected, this condition is most severe at the smallest angle θ where more of the radiated energy is incident upon the ground plane. The effect of the absorber in reducing the reflected signal can be observed.

B. Impedance

Swept frequency return loss measurements were performed on the slot array with and without polarizer (see Fig. 20). Maximum VSWR over the frequency

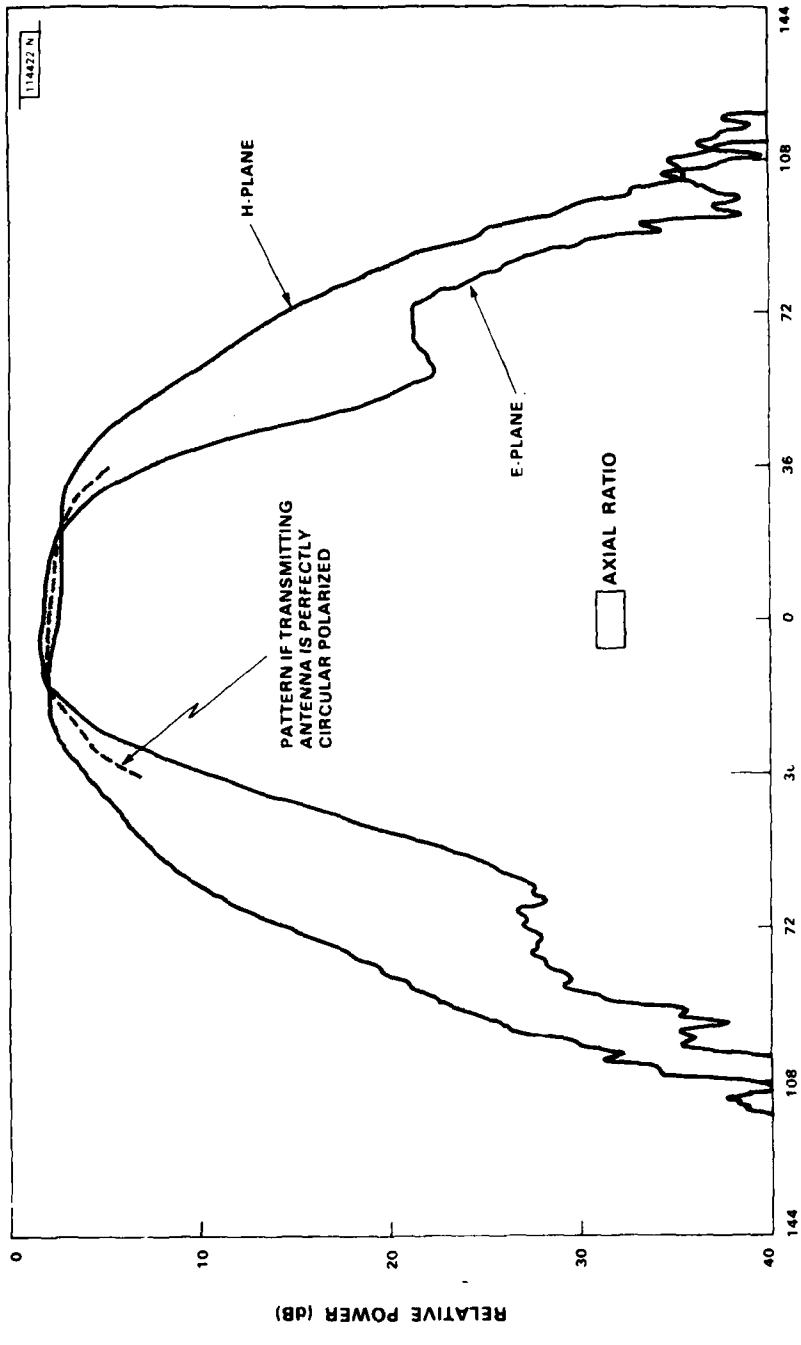

Fig. 16. Typical vertical polarization pattern - circularly polarized array.

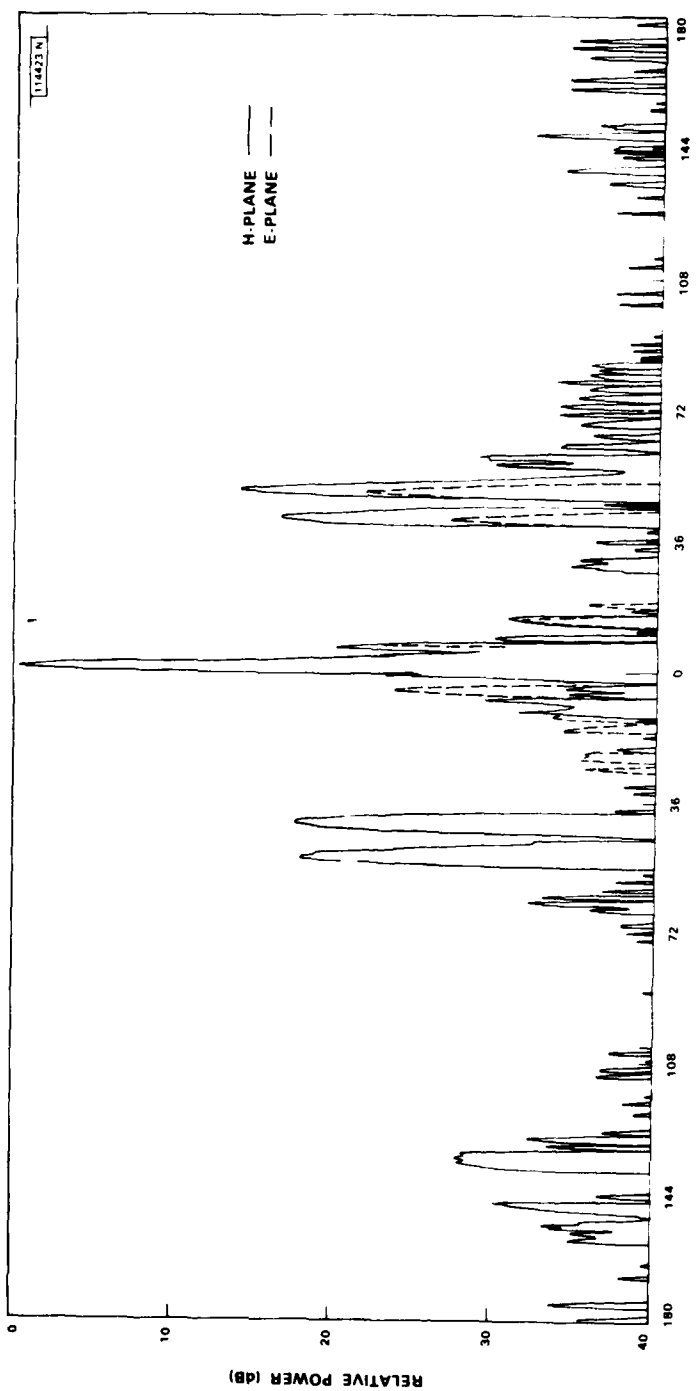

Fig. 17. Typical azimuth polarization pattern - circularly polarized array.

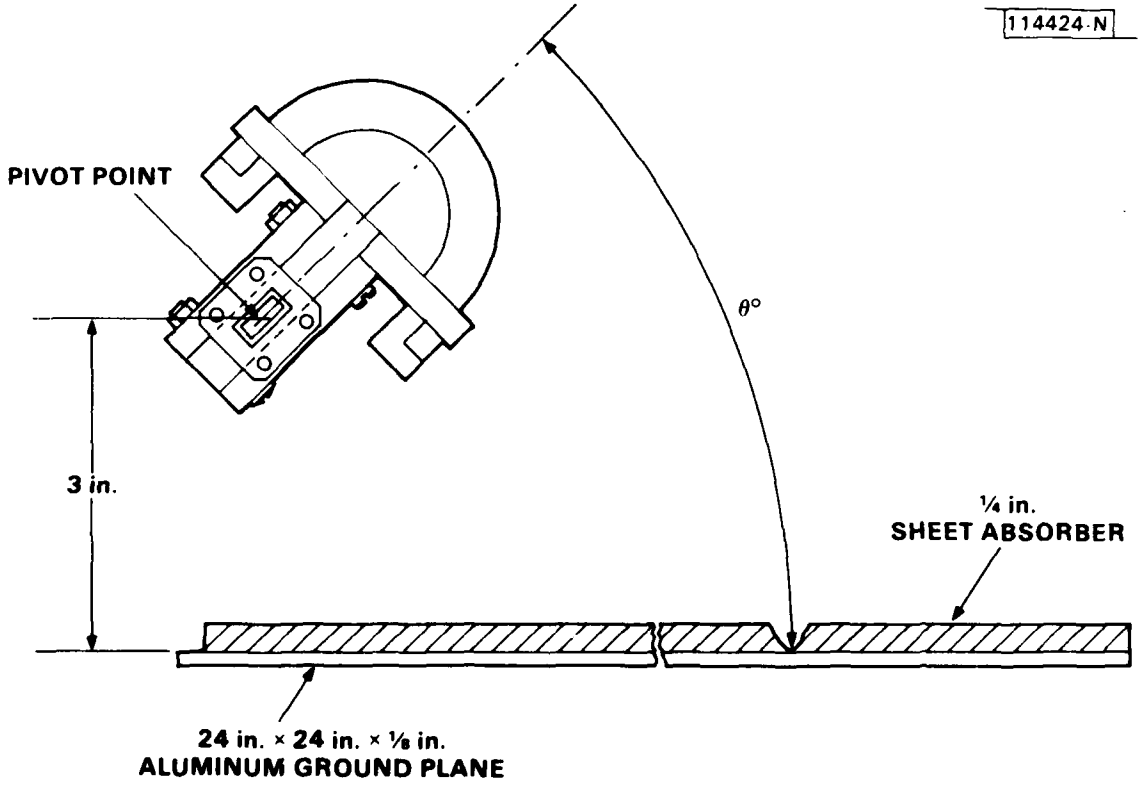

Fig. 18. Sketch of circularly polarized array over ground plane.

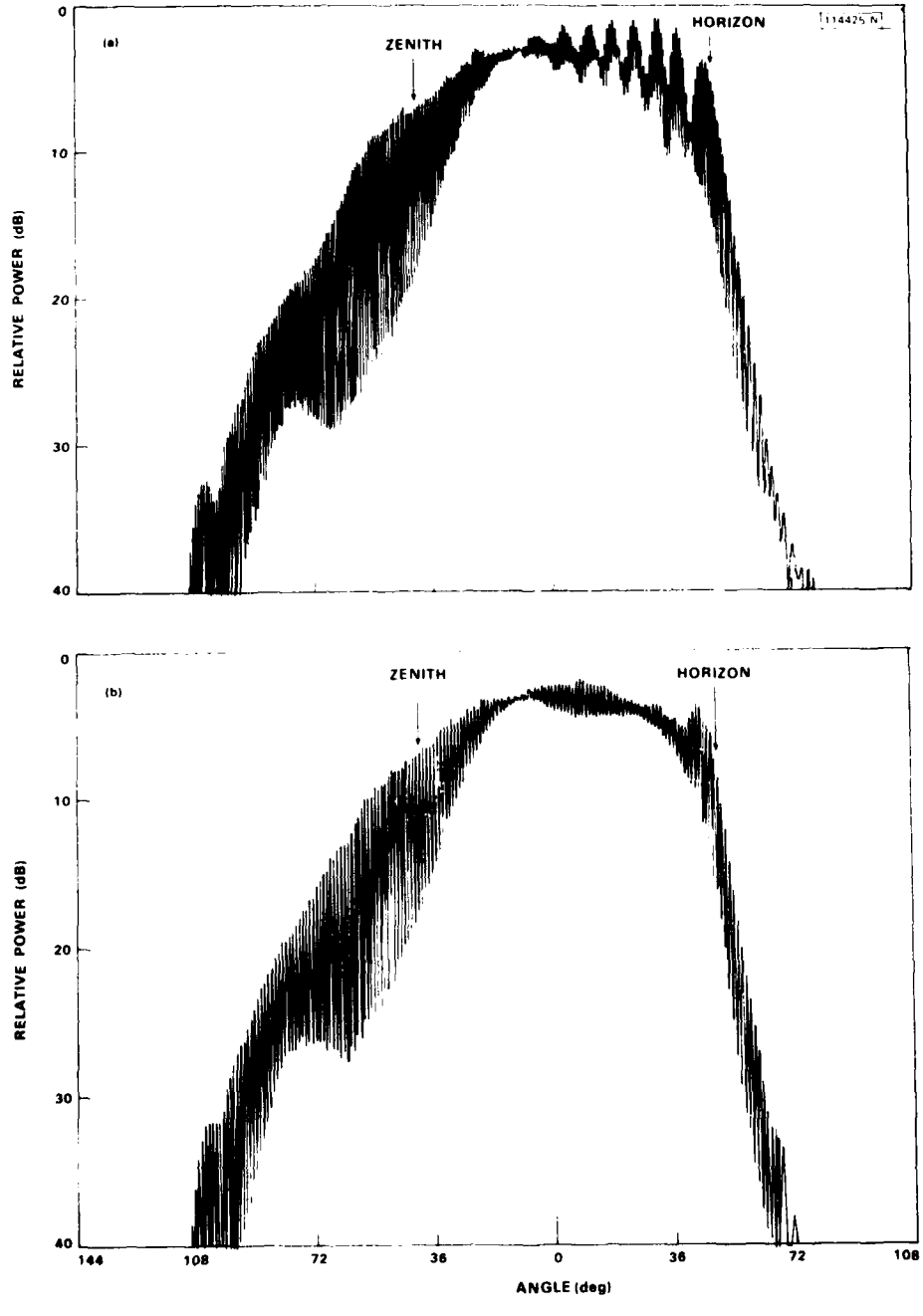

Fig. 19. Array over ground plane, θ=45°: (a) without absorber, (b) with absorber.

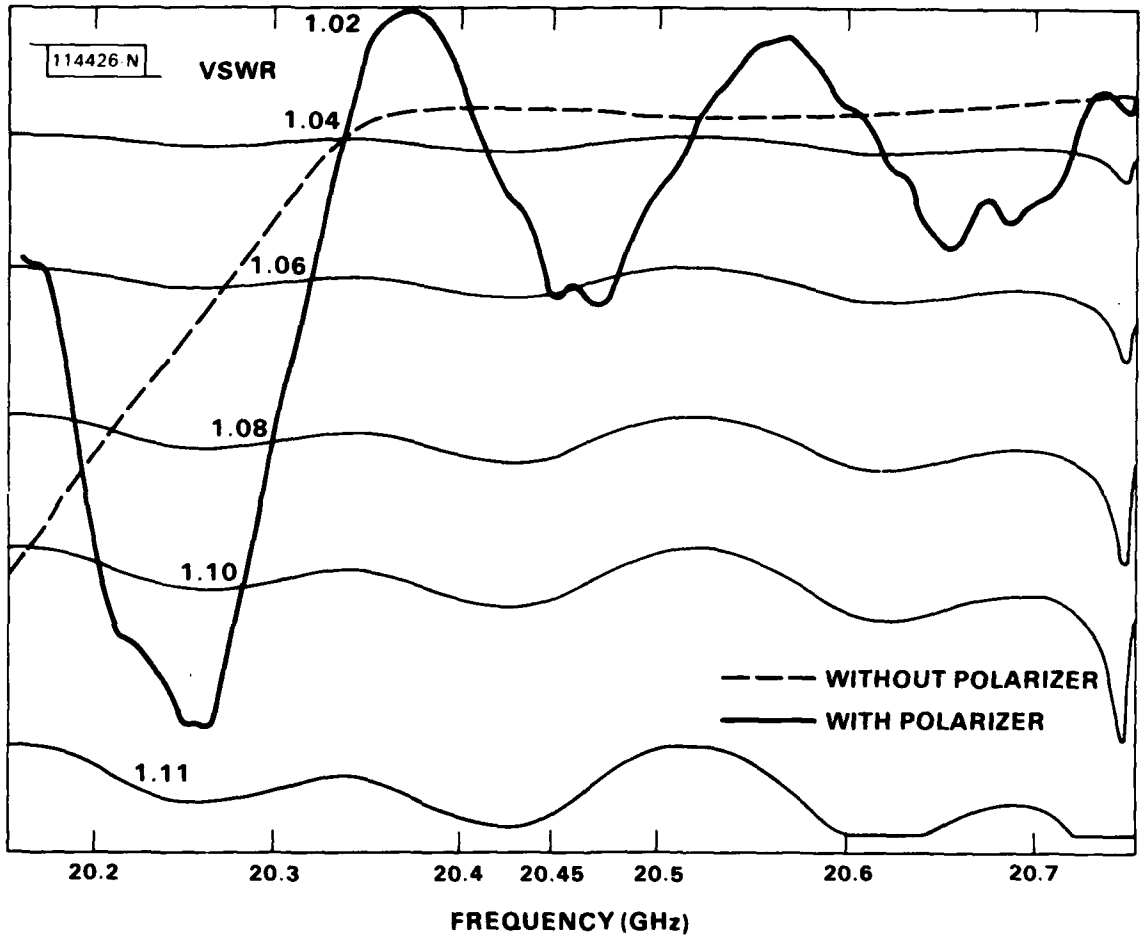

Fig. 20. VSWR - linear and circularly polarized array.

band is 1.07 without the polarizer and 1.11 with the polarizer. In either case the impedance match is well within the design goal.

C. Gain

The gain measurements were conducted using the substitution technique, where a linearly polarized standard gain horn is compared with the array in a linearly polarized field from the source antenna. The measured on-axis gain at 20.45 GHz without the polarizer is approximately 24.0 dBi, which computes to an efficiency of approximately 60%. Considering the tapered amplitude distribution, the measured gain is within reason.

The gain of the circularly-polarized array, which is computed for a perfectly circularly-polarized source, is 22.0 dBi at 20.45 GHz. The gain of the array with polarizer is approximately 1.8 dB lower than the gain without polarizer.

IV. CONCLUSIONS

A summary of the performance of an EHF waveguide slot array follows: measurements conducted over the frequency band revealed: gain is greater than or equal to 22.0 dBi, E-plane half power beamwidth is 1.56°, and H-plane half power beamwidth is 65°. Except for the first sidelobe and the cross polarized grating lobes at approximately 45°, the sidelobe levels are less than -30 dB and typically less than 40 dB from the peak of the main lobe. These results agree reasonably well with the computed theoretical values.

The measured results on the array give realistic figures on which to evaluate its performance as a paging antenna. Further refinements could yield somewhat improved performance. Improvements in the polarizer could perhaps increase the gain by as much as 1.8 dB, up to the linearly polarized level, and reduce the sidelobe levels. The unwanted cross-polarized component might also be suppressed by means of a spatial filter. Finally, the ground plane interference effect could also be investigated further to find a practical means of attenuating the reflected signal from the ground plane.

ACKNOWLEDGMENTS

The author is grateful to Dr. Alan J. Simmons and Walter Rotman for their assistance and guidance in the development effort and to Mr. John Russo for the RF testing and careful documentation of the measurements performed on this device.

REFERENCES

1. H. Jasik, Antenna Engineering Handbook, (McGraw-Hill, New York, 1961) pp. 9-13.

2. W. Watson, Waveguide Transmission and Antenna Systems, (Oxford, New York, 1947) p. 87.

3. H. Jasik, loc cit., pp. 2-22.

4. Ibid, pp. 9-16.

5. Ibid, pp. 17-20.

6. A. F. Harvey, Microwave Engineering, (Academic Press, New York, 1963) p. 656.

UNCLASSIFIED

SECURITY CLASSIFICATION OF THIS PAGE *(When Data Entered)*

REPORT DOCUMENTATION PAGE		READ INSTRUCTIONS BEFORE COMPLETING FORM
1. REPORT NUMBER ESD-TR-82-001	2. GOVT ACCESSION NO. AD-A114291	3. RECIPIENT'S CATALOG NUMBER
4. TITLE *(and Subtitle)* A 20 GHz Circularly Polarized, Fan Beam Slot Array Antenna		5. TYPE OF REPORT & PERIOD COVERED Technical Report 6. PERFORMING ORG. REPORT NUMBER Technical Report 563
7. AUTHOR(s) Dennis C. Weikle		8. CONTRACT OR GRANT NUMBER(s) F19628-80-C-0002
9. PERFORMING ORGANIZATION NAME AND ADDRESS Lincoln Laboratory, M.I.T. P.O. Box 73 Lexington, MA 02173-0073		10. PROGRAM ELEMENT, PROJECT, TASK AREA & WORK UNIT NUMBERS Program Element No. 33142A
11. CONTROLLING OFFICE NAME AND ADDRESS U.S. Army Satellite Communications Agency Ft. Monmouth, NJ 07703		12. REPORT DATE 9 March 1982 13. NUMBER OF PAGES 40
14. MONITORING AGENCY NAME & ADDRESS *(if different from Controlling Office)* Electronic Systems Division Hanscom AFB, MA 01731		15. SECURITY CLASS. *(of this report)* Unclassified 15a. DECLASSIFICATION DOWNGRADING SCHEDULE

16. DISTRIBUTION STATEMENT *(of this Report)*

Approved for public release; distribution unlimited.

17. DISTRIBUTION STATEMENT *(of the abstract entered in Block 20, if different from Report)*

18. SUPPLEMENTARY NOTES

None

19. KEY WORDS *(Continue on reverse side if necessary and identify by block number)*

EHF	slot array	ground mobile terminals
jammers	fan beam	paging antenna

20. ABSTRACT *(Continue on reverse side if necessary and identify by block number)*

An EHF waveguide slot array was developed for possible use as a receive-only paging antenna for ground mobile terminals. The design, fabrication, and measured performance of this antenna are presented. The antenna generates a circularly polarized fan beam that is narrow in azimuth and broad in elevation. When mechanically rotated in azimuth, it can receive a 20-GHz satellite transmission independent of mobile terminal direction. Azimuth plane sidelobe levels, which are typically < -40 dB from the main lobe, provide for discrimination against ground and airborne jammers.

DD FORM 1 JAN 73 1473 EDITION OF 1 NOV 65 IS OBSOLETE

UNCLASSIFIED

SECURITY CLASSIFICATION OF THIS PAGE *(When Data Entered)*

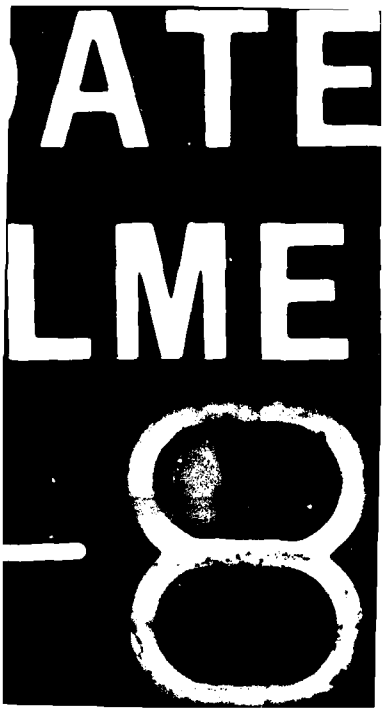
ATE
LME
8